Microbiology (2012), **158**, 1593–1606 **DOI** 10.1099/mic.0.055012-0

A Toll/interleukin (IL)-1 receptor domain protein from *Yersinia pestis* interacts with mammalian IL-1/Toll-like receptor pathways but does not play a central role in the virulence of *Y. pestis* in a mouse model of bubonic plague

Abigail M. Spear,[1] Rohini R. Rana,[2] Dominic C. Jenner,[1] Helen C. Flick-Smith,[1] Petra C. F. Oyston,[1] Peter Simpson,[2] Stephen J. Matthews,[2] Bernadette Byrne[2] and Helen S. Atkins[1]

Correspondence
Abigail M. Spear
amspear@dstl.gov.uk

[1]Biomedical Sciences Department, Defence Science and Technology Laboratory, Porton Down, Salisbury SP4 0JQ, UK

[2]Division of Molecular Biosciences, Imperial College London, London SW7 2AZ, UK

Received 26 September 2011
Revised 27 February 2012
Accepted 6 March 2012

The Toll/interleukin (IL)-1 receptor (TIR) domain is an essential component of eukaryotic innate immune signalling pathways. Interaction between TIR domains present in Toll-like receptors and associated adaptors initiates and propagates an immune signalling cascade. Proteins containing TIR domains have also been discovered in bacteria. Studies have subsequently shown that these proteins are able to modulate mammalian immune signalling pathways dependent on TIR interactions and that this may represent an evasion strategy for bacterial pathogens. Here, we investigate a TIR domain protein from the highly virulent bacterium *Yersinia pestis*, the causative agent of plague. When overexpressed *in vitro* this protein is able to downregulate IL-1β- and LPS-dependent signalling to NFκB and to interact with the TIR adaptor protein MyD88. This interaction is dependent on a single proline residue. However, a *Y. pestis* knockout mutant lacking the TIR domain protein was not attenuated in virulence in a mouse model of bubonic plague. Minor alterations in the host cytokine response to the mutant were indicated, suggesting a potential subtle role in pathogenesis. The *Y. pestis* mutant also showed increased auto-aggregation and reduced survival in high-salinity conditions, phenotypes which may contribute to pathogenesis or survival.

INTRODUCTION

The Toll/interleukin (IL)-1 receptor (TIR) domain was first recognized as a stretch of sequence homology spanning approx. 160 aa, common to the cytoplasmic domains of the Toll receptor from *Drosophila* and the mammalian IL-1 receptor (IL-1R) (Gay & Keith, 1991; Sims *et al.*, 1988). A homologous human receptor was identified and subsequently 'Toll-like receptors' (TLRs) were found across mammalian species (Medzhitov *et al.*, 1997). TLRs belong to a wider class of proteins, the Toll/IL-1 superfamily, characterized by the presence of a large extracellular leucine-rich repeat domain and an intracellular TIR domain linked by a single transmembrane region. TLRs are suggested to signal as oligomers (Latz *et al.*, 2007; Triantafilou *et al.*, 2006). Upon interaction with a pathogen-associated molecular pattern, TLRs are thought to undergo a molecular rearrangement of the intracellular TIR domains to generate an active interaction domain. This in turn allows recruitment of intracellular adaptor proteins through heterotypic TIR interactions, stimulation of intracellular signalling pathways and ultimately activation of the innate immune system. The TIR domain therefore plays a pivotal role in signalling from these receptors and their importance in immune regulation has made them the subject of intense study (Monie *et al.*, 2009; O'Neill & Bowie, 2007).

Proteins containing TIR domains are found across eukaryotic species, and Newman *et al.* (2006) identified over 200 proteins containing putative TIR domains in bacterial species using a bioinformatic search. Further studies on the TIR domain protein (Tdp) from *Salmonella enteritidis* (TlpA) and, more recently, Tdps from *Brucella melitensis* and a uropathogenic strain of *Escherichia coli*

Abbreviations: BME, β-mercaptoethanol; CI, competitive index; HPI, high pathogenicity island; IL, interleukin; IL-1R, IL-1 receptor; MLD, median lethal dose; SEAP, secreted alkaline phosphatase; Tdp, TIR domain protein; TIR, Toll/IL-1 receptor; TLR, Toll-like receptor.

(TcpB/Btp1 and TcpC, respectively) have suggested that bacterial Tdps have a role in the subversion of mammalian TLR signalling via their interaction with host TIR domain-containing proteins (Cirl *et al.*, 2008; Newman *et al.*, 2006; Radhakrishnan *et al.*, 2009; Salcedo *et al.*, 2008; Yadav *et al.*, 2010). Our more recent bioinformatic survey identified over 900 Tdps in both 'pathogenic' and 'non-pathogenic' bacterial species (Spear *et al.*, 2009), questioning the proposed 'subversion hypothesis' and suggesting that there may be alternative or additional functions for Tdps in bacteria. Although it seems likely that microbial TIR domains play a role in immune subversion in some bacterial species, it is also possible that the domains also have other roles.

During our survey, a Tdp was identified in the Gram-negative bacterium *Yersinia pestis*, a highly virulent pathogen responsible for the systemic disease plague, of which there have been three pandemics throughout history (Perry & Fetherston, 1997). *Y. pestis* is primarily a rodent pathogen but also readily infects humans and is normally transmitted subcutaneously via the bite of an infected flea or via inhalation, particularly during a pandemic (Perry & Fetherston, 1997). *Y. pestis* is closely related to *Yersinia pseudotuberculosis* but with some significant adaptations (Hinnebusch, 2005). For example, *Y. pseudotuberculosis* is a mammalian enteropathogen widely found in the environment whereas *Y. pestis* is a blood-borne mammalian pathogen that is able to parasitize insects but does not survive well in the environment. Horizontally acquired DNA is likely to have been significant in having enabled *Y. pestis* to adapt to new hosts and indeed *Y. pestis* contains three regions of unusual GC bias, usually caused by the very recent acquisition of DNA (e.g. from a prophage) or by the inversion or translocation of blocks of DNA (Zhou & Yang, 2009).

After infection with *Y. pestis*, bacterial replication occurs first at the site of infection, but subsequently the bacteria enter the lymphatic system via a mechanism of uptake and survival within macrophages, allowing them to spread to the lymph nodes and then into the bloodstream and organs such as the spleen and liver. Extensive replication within these organs occurs whereby bacteria return to the bloodstream and the host finally dies of septicaemic shock (Lukaszewski *et al.*, 2005). All three of the human pathogenic *Yersinia* sp. carry a 70 kb plasmid denoted the plasmid of *Yersinia* virulence (pYV in *Y. pseudotuberculosis*, pCD1 in *Y. pestis*) required for replication in lymphoid tissues, for which *Yersinia* have a tropism (Balada-Llasat & Mecsas, 2006). As *Y. pestis* is a highly pathogenic bacterial species already known to engage in subversion of TLR signalling, our aim in this study was to evaluate the role of *Y. pestis* Tdp (YpTdp) in immune system evasion using a cell-based model system of NFκB activation and construction, and evaluation of a *Y. pestis* YpTdp-deficient mutant.

METHODS

Animals. All animal studies were carried out in accordance with the UK Scientific Procedures Act (1986). Animal handling and infection studies were carried out by trained staff at Dstl. Pathogen-free 6- to 8-week-old female BALB/c mice were obtained from Charles River Laboratories and housed in high-efficiency particulate air-filtered barrier units. Challenge studies were performed in a custom-built animal containment level 3 rigid wall isolation unit. Mice were acclimatized for at least 7 days prior to initiation of procedures. Mice were given food and water *ad libitum* and were kept at 25 °C with alternating 12 h periods of light and dark. Animals that had reached the humane end-point described in the UK Home Office project licence used for this work were killed by cervical dislocation.

Generation of expression constructs. The *Y. pestis* ORF YPO1883 (termed *YpTdp*) was amplified from *Y. pestis* CO92 genomic DNA with primers incorporating the CACC motif necessary for directional TOPO cloning into the mammalian expression vector pcDNA3.2. The primers used were 5′-CACC**ATG**GCAAGCTGCATCCC-3′ (sense) and 5′-GGGCACAATCTTGTTTACAGTCTCGATAAAT-3′ (antisense). The CACC motif is underlined and the start codon is denoted in bold. The stop codon was removed to allow expression of a C-terminal V5 tag on the expression vector. DNA encoding only the TIR domain from YpTdp (termed YpTIR) was also amplified from *Y. pestis* CO92 genomic DNA with the strategy above using primers 5′-CACCTCCATCTGGAAGCCAAATTTAATTCG-3′ (sense) and 5′-GGCTTCATCAAAACTCTGAGATGC-3′ (antisense). The resulting *YpTdp* and *YpTIR* fragments were ligated into the dTOPO cloning site in pcDNA3.2. The gene fragment coding for the YpTIR was also cloned into the Gev2 expression vector (Huth *et al.*, 1997) as described previously (Rana *et al.*, 2011). The resulting expression construct contains an N-terminal GB1 tag and a C-terminal 6His tag (GB1-YpTIR-His). The Pro173His mutant YpTIR and YpTdp were generated using a QuikChange mutagenesis kit (Stratagene). The MyD88TIR-GST was generated by cloning the gene fragment coding for residues T148 to P296 into pGEX-5x-2 (GE Healthcare). All constructs were transformed into the BL21(DE3) Star expression strain (Stratagene).

Reporter assays. For luciferase reporter assays, HEK293H cells (2×10^4 cells per well) were seeded into 96-well plates and transfected 24 h later with expression vectors and luciferase reporter vectors using Genejuice (Novagen). In all cases, 60 ng per well of an NFκB-luciferase reporter vector (a kind gift from Professor Andrew Bowie, Trinity College, Dublin, Ireland) was transfected for quantification of NFκB activity and 20 ng per well of phRL-TK reporter gene (Promega) to normalize data for transfection efficiency. The total amount of DNA per transfection was kept constant at 230 ng by addition of 'empty vector' DNA in the form of the control vector pcDNA3.2_Cat expressing the chloramphenicol acetyltransferase enzyme (Invitrogen). Preliminary investigations found that the expression of chloramphenicol acetyltransferase had no effect on reporter expression (data not shown). Twenty-four hours after transfection, the cells were stimulated with IL-1β or tumour necrosis factor α (TNF-α) at 100 ng ml^{-1} (or PBS as control) for 6 h before the cells were harvested and reporter activity was measured using a Luminoskan Ascent microplate luminometer (ThermoFisher). Data are expressed as the percentage induction relative to stimulated cells in the absence of YpTdp/YpTIR (mean $\pm$ SEM) relative to control levels, for five separate experiments each with a minimum of three experimental replicates.

For SEAP (secreted alkaline phosphatase) reporter assays downstream of TLR4, HEK-Blue hTLR4 cells (InvivoGen) were seeded in six-well plates at approximately 1.5×10^6 cells per well and transfected 24 h later with 4 μg Tdp-expression vectors using Lipofectamine 2000 (Invitrogen). Transfection of reporter vectors was not required in this case as a SEAP reporter is already present within the cells. Cells were harvested 24 h later and 5×10^4 cells per well were seeded in a 96-well plate containing 1 μg LPS ml^{-1} (or PBS for unstimulated cells). After

24 h, 40 µl media was removed from these cells and added to 160 µl Quanti-Blue (InvivoGen). Reporter activity (A_{620}) was measured 30–90 min post-incubation with Quanti-Blue. Data are expressed as the percentage induction relative to stimulated cells in the absence of YpTdp/YpTIR/YpTdp-P173H (mean ± SEM) relative to control levels, for three separate experiments each with three experimental replicates.

ELISA. For determination of IL-8 concentrations in cell supernatants, a BD OptEIA Set Human IL-8 was used according to the manufacturer's instructions. The absorbance from each well was measured at 450 nm using a ThermoFisher microplate reader. Standard curves were constructed relating IL-8 concentrations to absorbance at 450 nm and were used to determine IL-8 concentrations.

GST pull-down assays. The native and Pro173His mutant forms of GB1-YpTIR-His were purified using Co^{2+}-immobilized metal affinity chromatography (Qiagen). The proteins were eluted in buffer [20 mM HEPES-NaOH (pH 8), 250 mM NaCl, 150 mM imidazole]. The GST-MyD88-TIR construct was purified using immobilized glutathione resin and remained bound to the column as the 'bait' protein. The purified YpTIR proteins were individually loaded onto the GST-MyD88-TIR column and the resin was incubated at 4 °C for 1 h. The column was washed using buffer [20 mM Tris/HCl (pH 7), 150 mM NaCl, 2 mM β-mercaptoethanol (BME)]. The bound proteins were eluted with buffer [50 mM Tris/HCl (pH 8), 10 mM glutathione, 2 mM BME] and concentrated threefold using a 10 kDa molecular mass cut-off filter (Millipore). The samples were analysed by Western blot using both anti-GST (Merck) and anti-His (Sigma-Aldrich) antibodies.

Generation of the *Y. pestis YpTdp* deletion mutant. A genetic knockout of the gene encoding YpTdp was achieved using the 'lambda (λ) red swap' method of Datsenko & Wanner (2000). The kanamycin resistance cassette (Kan^R) was amplified by PCR from the vector pK2 (Taylor *et al.*, 2005) (Professor P. C. F. Oyston, Dstl, UK) using 70 nt primers containing 50 nt of DNA flanking either side of the *YpTdp* gene: sense, 5′-CAATAACCAATCAAAGCTCACTCAAAGAAGCCACTAAGAGGGACATTATG **GATCTGCCACGTTGTGTCTC**; anti-sense, 5′-ATTTGCCTGTCTCCGTTGTTGGAGTGAAGATATCAAAAACAGGCAATTA**GCTCTGCCAGTGTTACAACC**. The bases corresponding to Kan^R are in bold and the start and stop codons from the *YpTdp* gene are underlined. This PCR product was digested with *Dpn*I to remove contaminating plasmid template and electroporated into *Y. pestis* GB containing the recombinase helper plasmid pAJD434 (Maxson & Darwin, 2004) (Dr D. Ford, Dstl, UK). Bacterial colonies were screened for their ability to grow on media containing kanamycin, and by PCR using primers outside of the gene of interest in order to observe a size difference in the PCR product of the mutant (the Kan^R product is 1231 bp, *YpTdp* is 1338 bp). A confirmatory PCR was also carried out with a kanamycin-specific PCR primer, giving a positive result only on mutant colonies. Once a potential *YpTdp* mutant was identified, the helper recombinase plasmid was cured by growth of the strain at 37 °C. Loss of the recombinase plasmid was confirmed by the loss of PCR products corresponding to the *exo* and *gam* genes from the helper plasmid. The presence of the *Y. pestis* virulence plasmid (pCD1) was confirmed by PCR amplification of the *yscC* gene from this plasmid. The replacement of the *YpTdp* gene with a kanamycin cassette was confirmed by amplifying the new insert using PCR, cloning this product into pCR2.1 (Invitrogen) and subsequent sequencing of this construct.

Surface hydrophobicity. The hydrophobicity of bacterial strains was measured using the bacterial adhesion to hydrocarbon test (Beck *et al.* 1988; Rosenberg, 1984). Overnight cultures were diluted 1 : 10 in blood agar base (BAB) broth and grown at 28 °C with orbital shaking. At defined time points, 2 ml culture was removed, washed twice in PBS and resuspended to an OD_{590}~1.0. Subsequently, 2 ml of this suspension was overlaid with 600 µl n-hexadecane (Sigma-Aldrich) and vortexed for 1 min. The phases were allowed to separate for 15 min at room temperature and the percentage of culture partitioning in the hydrocarbon phase was calculated as follows:

$\{[OD_{590}(\text{original bacterial suspension}) - OD_{590}(\text{aqueous phase})]/OD_{590}(\text{original bacterial suspension})\} \times 100$

Sedimentation assay. Overnight cultures of *Y. pestis* were set up and grown for 16–18 h at 28 °C with orbital shaking. The cultures were then diluted 1 : 10 in BAB broth and shaken at 28 °C for 4 h. At this point 3 ml culture was transferred to a cuvette and left to stand at room temperature. The OD_{590} was recorded at different time points. In this experiment, if the bacteria auto-aggregate, they settle and the supernatant clears, leading to an OD_{590} decrease.

MIC assay. Polymixin B was appropriately diluted in sterile BAB broth to give a stock concentration of 250 µg ml^{-1}. This was doubly diluted across the rows of a 96-well microtitre plate in triplicate to give a final volume of 100 µl in each well. A row of wells with no polymixin B were included as a positive control for bacterial growth. A row of wells with broth only served as a negative control. Then, 100 µl of a solution of 10^5–10^6 c.f.u. *Y. pestis* ml^{-1} was overlaid into the appropriate wells. Bacterial counts in this input culture were determined by enumeration on BAB agar plates. The plates were incubated at 28 °C and the OD_{600} was recorded at 24 h. The mean value from the negative control wells was subtracted from all other values and the percentage survival of bacteria in concentrations of polymixin B was calculated as follows:

(mean OD_{600} of experimental wells/mean OD_{600} of positive control wells) × 100

Salt shock. Overnight cultures were diluted 1 : 10 and grown to exponential phase (OD_{590}~0.3). Then, 100 µl culture was added to 10 ml filter-sterilized NaCl solution and incubated at 28 °C with orbital shaking for 3 h. This input culture was serially diluted and plated for enumeration of bacteria. The NaCl solutions were then serially diluted and plated for enumeration of bacteria. Percentage survival in NaCl was calculated as follows:

(c.f.u. in NaCl solution/c.f.u. in input culture) × 100

***In vivo* competitive index study.** Stationary phase overnight cultures of *Y. pestis* GB and *Y. pestis* Δ*YpTdp* were diluted 1 : 10 in BAB broth and incubated at 28 °C with shaking at 180 r.p.m. until the cultures reached an OD_{590} of 0.6. At this point, each culture was serially diluted to 10^{-4} in PBS. The 10^{-4} dilutions of each strain were then mixed at a 1 : 1 ratio and 100 µl of this solution was used to challenge six BALB/c mice via the intravenous route. After 48 h, the mice were killed by cervical dislocation and their spleens were removed and placed in PBS. The spleens were immediately macerated through a 0.2 µm sieve in 3 ml PBS and this solution was serially diluted and plated onto BAB agar for enumeration of total *Y. pestis* and onto BAB agar containing 50 µg kanamycin ml^{-1} for enumeration of *Y. pestis* Δ*YpTdp*. *Y. pestis* Δ*YpTdp* plate counts were then subtracted from counts on BAB agar to calculate a ratio of wild-type to mutant bacteria in the spleen. A ratio of 5 : 1 (wild-type/mutant) was considered to indicate significant attenuation.

***In vivo* MLD study.** Overnight stationary phase cultures of *Y. pestis* GB and *Y. pestis* Δ*YpTdp* were diluted as for the competitive index study and allowed to grow to OD_{590} 0.6. At this point, the wild-type

culture was serially diluted to 10^{-7} (corresponding to approx. 1 c.f.u. per 100 µl) and the mutant culture was diluted to 10^{-8} (corresponding to approx. 0.1 c.f.u. per 100 µl). Then, 100 µl of the appropriate dilutions was used to inoculate six BALB/c mice by the subcutaneous route. The mice were then monitored twice daily and clinical scores/deaths were recorded. Mice were killed at a humane point by staff blinded to the project plan.

Colonization study. Overnight stationary phase cultures of *Y. pestis* GB and *Y. pestis* Δ*YpTdp* were diluted and allowed to grow to OD_{590} 0.6, which corresponds to approximately 10^8 c.f.u.; *Y. pestis* GB and *Y. pestis* Δ*YpTdp* cultures were then serially diluted to 10^{-7} and the −5, −6 and −7 dilutions were plated to determine exact c.f.u. counts. Then, 100 µl per mouse of the −5 dilution was used as the inoculum, giving an approximate dose of 100 c.f.u. per mouse. Eight groups of six BALB/c mice were inoculated via the subcutaneous route with approx. 100 c.f.u. of *Y. pestis* GB or *Y. pestis* Δ*YpTdp*. At 48, 72, 96 and 120 h one group of *Y. pestis* GB and one group of *Y. pestis* Δ*YpTdp* mice were culled and their blood and spleen were removed for bacteriological and immunological analysis. Spleen and blood were homogenized through a sterile 0.2 µm cell sieve into 1 ml sterile PBS before 100 µl was serially diluted further and plated out onto BCGA + glucose media. Plates were incubated at 28 °C for 48 h before being counted. Calculations were completed to give the number of c.f.u. ml^{-1} for each mouse.

Cytokine analysis was completed by taking 200 µl of organ homogenate and centrifuging for 5 min at 200 ***g***. Supernatants were collected and processed for cytokine content using a Becton Dickinson Cytometric Bead Array, with assays read on a FACs CANTO II flow cytometer. The assay was carried out according to the manufacturer's instructions. Final samples were kept in 4 % paraformaldehyde for 24 h before being released for FACs analysis.

RESULTS

Bioinformatic characterization of the TIR domain protein from *Y. pestis*

All *Y. pestis* strains studied previously in our bioinformatic survey (Spear *et al.*, 2009) possess one protein that contains a TIR domain (herein denoted YpTdp, equivalent to *y2426* in *Y. pestis* KIM) (Deng *et al.*, 2002). This 358 aa protein exists, and is highly homologous, in all *Y. pestis* strains present in the NCBI non-redundant database and is annotated as a hypothetical protein. An identical protein is found in *Y. pseudotuberculosis* YPIII and a highly similar protein (89 % identical) is found in *Yersinia enterocolitica*. The *YpTdp* gene sits in one of the three regions of low GC content in the *Y. pestis* genome, next to the so-called high pathogenicity island (HPI) within the pigmentation (*pgm*) locus (Schubert *et al.*, 2004). This area of DNA encodes genes shown to be important for transmission of *Y. pestis* by the flea vector, and for the acquisition of iron from its mammalian host (Buchrieser *et al.*, 1998). The HPI is considered likely to have been acquired as a whole section from a bacteriophage (Buchrieser *et al.*, 1998). Interestingly, *YpTdp* is also present in a region flanked by an integrase, transposase and attB site and so may also be of phage origin.

Fig. 1 shows a multiple sequence alignment of the TIR domain from YpTdp with a variety of eukaryotic TIR domains. It is clear that the TIR domain from YpTdp shares homology in regions important for the definition and function of eukaryotic TIR domains, including homology in 'Box 1' and in the βC helix. However, differences are also clear: YpTdp lacks the conserved 'Box 2' motif RDxxPG (Xu *et al.*, 2000), although it does contain the conserved proline residue demonstrated to be important for eukaryotic TLR signalling function (Poltorak *et al.*, 1998). YpTdp also lacks a 'Box 3' motif, although the importance of this region for TIR domain function is less clear (Spear *et al.*, 2009; Xu *et al.*, 2000).

Effect of YpTdp on human IL-1/TLR signalling

To investigate the effect of the *Y. pestis* Tdp on mammalian immune signalling, the ORF encoding the protein was amplified from *Y. pestis* genomic DNA and cloned into a mammalian expression vector. The region of DNA encoding only the TIR domain from the protein (YpTIR, residues S130–A285), as predicted by alignment with structurally characterized TIR domains, was also amplified and cloned into this expression vector. Expression was confirmed from each construct in HEK293 cells by Western blotting (data not shown).

Using an *in vitro* cell-based assay the effect of YpTdp and YpTIR on IL-1/TLR4 signalling following exogenous stimulation was determined. The NFκB activation level in each case was assessed using NFκB reporter assays (Fig. 2). Expression of YpTdp or YpTIR had no effect on basal levels of reporter gene expression (data not shown). In all cases NFκB activity induced by each stimulant was normalized to 100 % and NFκB activity in the presence of YpTdp/YpTIR was expressed as a percentage of this. These data show that in the presence of YpTdp, IL-1β-induced NFκB activity was reduced to 53 % of control signalling ($P=0.0036$, column *t*-test) but that no such reduction was observed when the YpTIR domain was expressed (Fig. 2a). Similarly, LPS-induced signalling to NFκB in the presence of YpTdp was 83 % of control signalling ($P=0.0323$, column *t*-test), but YpTIR had no effect (Fig. 2c). In contrast, neither YpTdp nor YpTIR had any measurable effect on TIR-independent TNFα-induced signalling to NFκB (Fig. 2b). These results suggest that YpTdp is acting specifically on TIR domain-dependent signalling but that these effects are abolished when the TIR domain is expressed alone.

The effect of full-length YpTdp on IL-1β signalling was confirmed by analysing IL-8 in the media from the reporter assays, and via the IL-1β-induced degradation of IκBα over time (Fig. 3). IL-8 secretion induced by IL-1β signalling was reduced in the presence of YpTdp but restored in the presence of YpTIR, following the pattern of induced NFκB activity (Fig. 3a, b). The effect of YpTdp was also clear when the degradation of IκBα after IL-1β stimulation was monitored (Fig. 3c). Not only did YpTdp slightly delay the time at which IκBα is at its lowest level in the cell, but the feedback loop, by which NFκB activation causes the production of IκBα, appeared to be reduced in the presence of YpTdp (Fig. 3c).

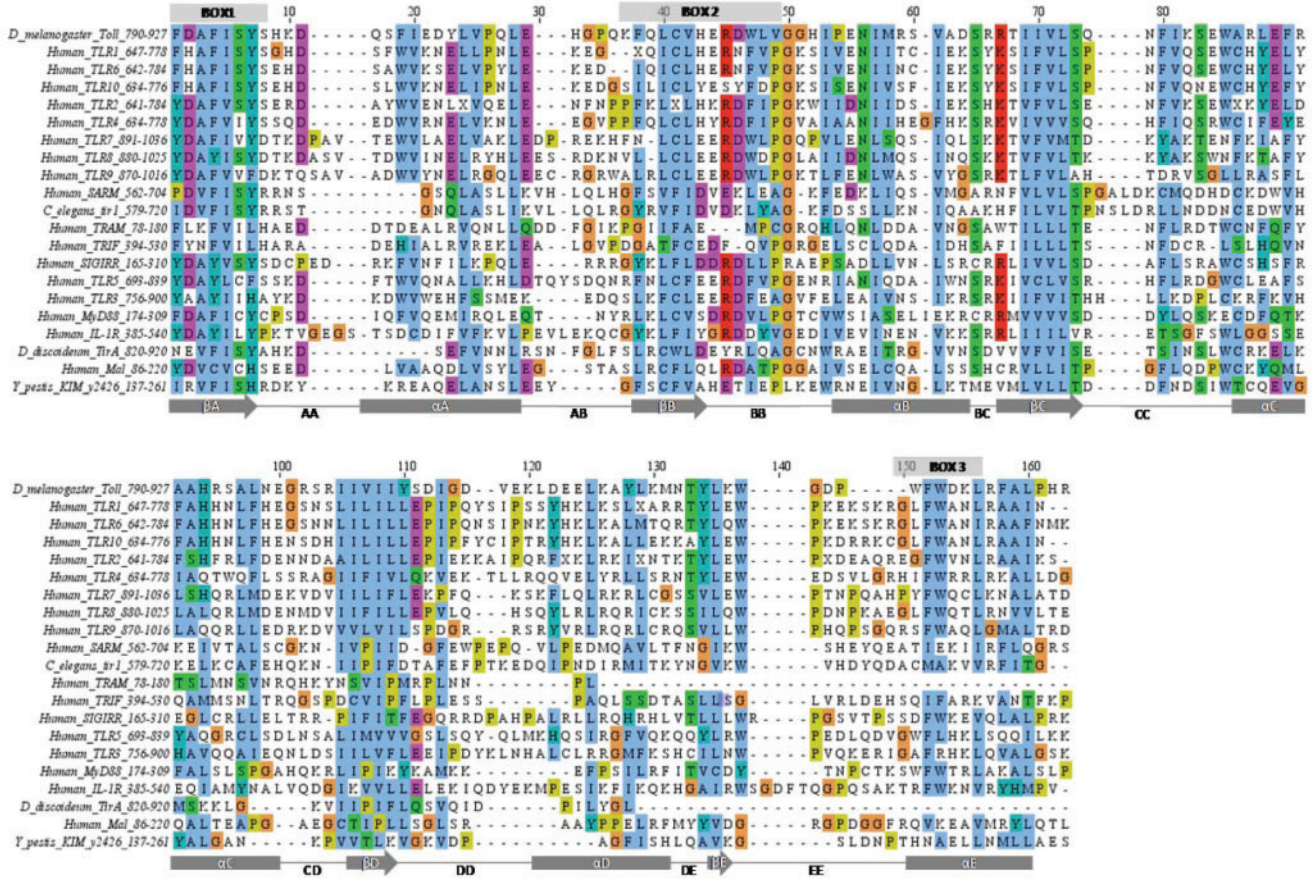

Fig. 1. Multiple sequence alignment of y2426 from *Y. pestis* KIM with eukaryotic TIR domain proteins. The multiple sequence alignment was carried out using the CLUSTALW2 algorithm on the EBI web server (http://www.ebi.ac.uk/tools/clustalw2) and coloured according to the CLUSTAL X colour scheme using Jalview editing software. TIR domain sequences were taken from *Homo sapiens*, *Caenorhabditis elegans*, *Dictyostelium discoideum* and *Drosophila melanogaster*. The grey boxes and arrows highlight regions of the YpTdp corresponding to the α-helix and β-sheet, respectively, as predicted by the 3D-Jury web server (http://meta.bioinfo.pl/submit_wizard.pl).

Interaction between YpTIR and MyD88 is dependent on Pro173

We wished to directly investigate the interaction between the YpTdp and the key human adaptor protein MyD88. However, it was not possible to express adequate amounts of soluble full-length YpTdp. Therefore, we investigated whether YpTIR (Rana *et al.*, 2011) expressed in *E. coli* interacts with human MyD88-TIR. The YpTIR was expressed in *E. coli* as a fusion protein with an N-terminal GB1 tag (the B1 immunoglobulin domain of streptococcal protein G). GST-tagged MyD88-TIR, also expressed in *E. coli*, was immobilized on glutathione resin and used as bait protein with the purified GB1-YpTIR-His used as prey. GST pull-down analysis indicated a specific interaction between YpTIR and MyD88-TIR (Fig. 4a). No interaction was detected between GB1-YpTIR-His and GST only (control) or between GST-MyD88-TIR and GB1-SV40-His (a GB1-tagged control protein) (Fig. 4b).

Previous research on the TIR domain proteins of TLRs 1, 2 and 10 has indicated a key role for a proline residue located on the exposed BB loop in signalling and dimer formation (Nyman *et al.*, 2008; Xu *et al.*, 2000). To investigate whether the equivalent residue in YpTIR was important for interaction with MyD88-TIR, a Pro173His mutant was generated and expressed as a GB1 fusion protein. GST pull-down analysis showed that the Pro173His mutant of GB1-YpTIR-His did not interact with MyD88-TIR (Fig. 4c, d).

One-dimensional NMR analysis confirmed that both the wild-type GB1-YpTIR-His and the Pro173His mutant are folded (Fig. 4e, f), strongly indicating that the lack of interaction observed between the Pro173His YpTIR and MyD88-TIR was not due to any disruption of the YpTIR domain structure introduced by the point mutation. These data further confirm the specificity of the interaction between the wild-type YpTIR and MyD88-TIR, indicating an important role for Pro173.

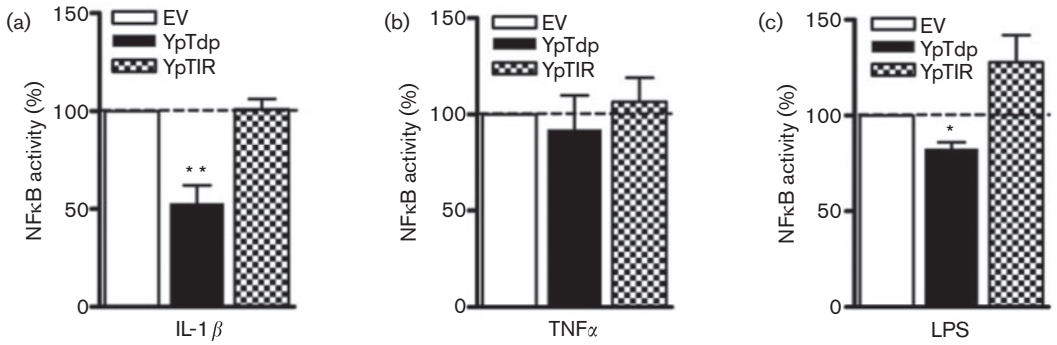

Fig. 2. Effect of YpTdp and YpTIR on human IL-1 and TLR4 signalling. (a, b) HEK293 cells were transfected with vectors expressing YpTdp (150 ng) or YpTIR (150 ng) along with reporter plasmid pNFκB-luc (60 ng) and reporter plasmid pRL-TK (20 ng). At 24 h post-transfection the cells were stimulated with IL-1β (a) or TNF-α (b) at 100 ng ml^{-1} and luciferase activity was assayed after 6 h. (c) HEK-Blue hTLR4 cells containing an alkaline phosphatase NFκB reporter were transfected with either empty vector or vector expressing YpTdp/YpTIR and stimulated with *E. coli* LPS (1 μg ml^{-1}) for 24 h. All results are expressed as percentage NFκB activity relative to stimulated cells transfected with empty vector (100 %). *$P<0.05$, **$P<0.01$, column *t*-test.

The high-resolution structure of the dimer of TLR10-TIR (Nyman *et al.*, 2008) reveals that the equivalent Pro residue is located at the dimer interface. A further dimer structure of the TIR domain from the non-pathogenic bacterium *Paracoccus denitrificans* (PdTIR) indicates that the Pro is not involved in dimer formation but along with the remainder of the BB loop is exposed to the aqueous solvent. Previous work has indicated that YpTIR forms a dimer in solution (Rana *et al.*, 2011). Static-light scattering analysis of the Pro173His mutant of GB1-YpTIR-His indicates that the protein is also a dimer (Fig. 4g). Thus, the loss of interaction between the YpTIR Pro173His mutant is not due to the disruption of the dimer. These data suggest that the Pro173 residue together with the rest of the BB loop is possibly exposed to solvent, as seen in the PdTIR structure, and that this plays a key role in mediating interactions with the human adaptor MyD88. A Pro173His mutant of YpTdp was also unable to down-regulate LPS-induced TLR4 signalling (Fig. 4h), suggesting that interaction of YpTdp with MyD88 is important for the disruption of TLR4-mediated signalling by this protein.

Growth and virulence of *Y. pestis* Δ*YpTdp*

To evaluate the role of YpTdp in *Y. pestis* virulence, a deletion mutant was constructed in *Y. pestis* GB using the gene swap method of Datsenko & Wanner (2000). In a cell culture model of macrophage infection using a murine macrophage cell line (J774A.1) there was no measurable difference in cell uptake between wild-type *Y. pestis* GB and the Δ*YpTdp* mutant, or in the replication of each strain within these macrophages (data not shown). With no difference in uptake or replication occurring it was deemed that the likelihood of seeing important differences in cytokine production by these macrophages was unlikely.

The virulence of *Y. pestis* Δ*YpTdp* was assessed *in vivo* using a competitive index (CI) study to determine its ability to colonize the spleen in competition with wild-type *Y. pestis* GB, via assessment of its median lethal dose (MLD) in mice (Table 1) and its colonization of the spleen and blood over time (Fig. 5). Overall, the results from these *in vivo* infection experiments showed that *Y. pestis* Δ*YpTdp* did not have a reduced virulence phenotype when compared with wild-type bacteria. The MLD for *Y. pestis* Δ*YpTdp* was calculated using the Reed–Meunch equation (Reed & Muench, 1938) as 1.29 c.f.u., which is similar to the previously calculated MLD for *Y. pestis* GB (1 c.f.u.) (Robinson *et al.*, 2005). The mean CI for *Y. pestis* Δ*YpTdp* was 2.04; in line with other studies (Stubben *et al.*, 2009), a CI of $\leqslant 0.2$ was considered to reflect attenuation and thus *Y. pestis* Δ*YpTdp* was considered not attenuated. In the colonization studies there was no significant difference in the colonization of the spleen or blood by *Y. pestis* Δ*YpTdp* when compared with *Y. pestis* GB (Fig. 5). In addition, the numbers of monocytes, neutrophils and natural killer cells in the spleen or blood were not significantly different between mice administered with either the mutant or wild-type *Y. pestis* during the colonization study (data not shown). Similarly, levels of IL-6, TNFα and MCP-1 (monocyte chemotactic protein-1) in the spleens and blood of mutant and wild-type *Y. pestis*-infected mice were not significantly different during the time-course of infection. However, significant differences were found in levels of IL-12p70 in the spleen (Fig. 6a), IL-10 in the spleen (Fig. 6b) and interferon γ (IFNγ) in the blood (Fig. 6c).

Increased levels of IL-12 in the spleen at 72 and 96 h were observed during Δ*YpTdp* infection compared with wild-type infection (Fig. 6a). It is possible that wild-type *Y. pestis* is actively suppressing the levels of pro-inflammatory IL-12

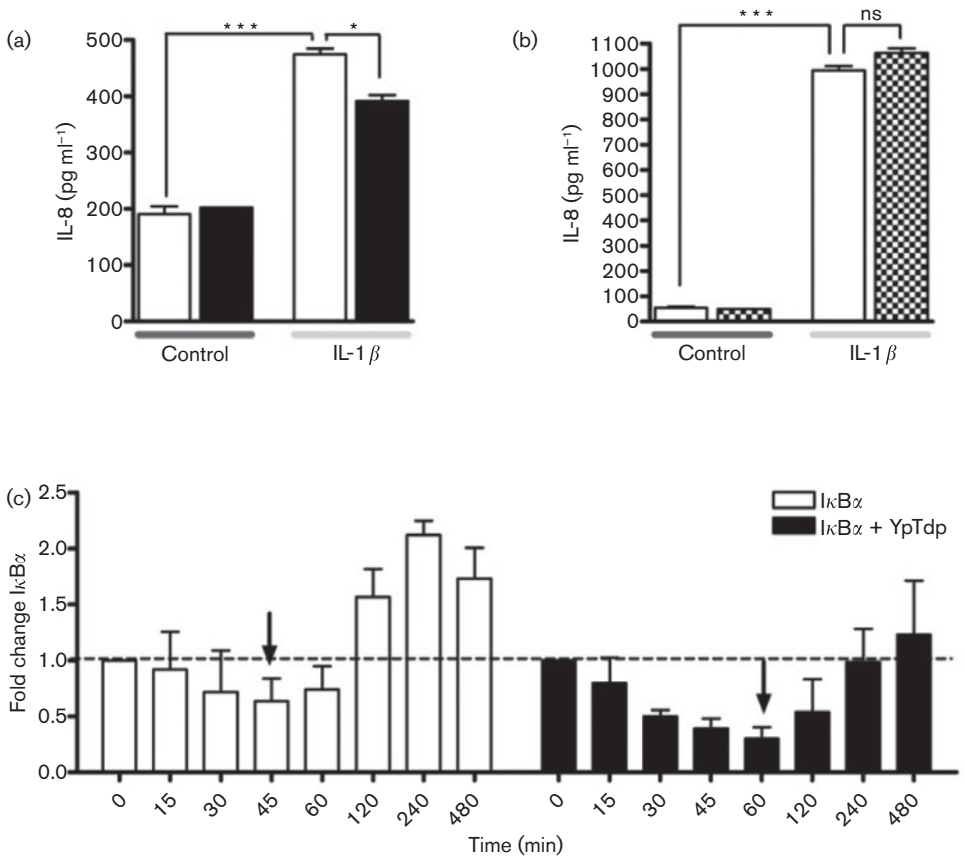

Fig. 3. Effect of YpTdp and YpTIR on IL-1 signalling. The figure shows IL-8 production by HEK293 cells stimulated with 100 ng IL-1β ml^{-1} in the presence and absence of YpTdp (a) and YpTIR (b) and the degradation of IκBα after stimulation with 100 ng IL-1β ml^{-1} in the presence and absence of YpTdp as monitored by Western blotting (c). The amount of IκBα was quantified using densitometry on the developed film and normalized to β-actin levels. Levels are expressed as fold difference from time zero. Open bars, levels of IκBα in the presence of control vector; filled bars, levels of IκBα in the presence of YpTdp. Arrows indicate the points at which the levels of IκBα are at their lowest compared with time zero. ns, Not significant; *P<0.05; **P<0.01; ***P<0.001.

via YpTdp and when this protein is removed, levels of IL-12 are increased. In a study in which mice were dosed with a TLR4 agonist prior to *Y. pestis* infection, increased levels of IL-12 were observed in addition to an increased level of survival (Airhart *et al.*, 2008), suggesting that IL-12 would be a target for active immune suppression through a TIR-dependent pathway. Increased levels of IL-10 were observed in the spleen at 72 h during Δ*YpTdp* infection compared with wild-type infection (Fig. 6b). IL-10 expression is generally considered to be associated with *Y. pestis* wild-type infection, particularly in the case of systemic infection. However, IL-10 is regulated by IL-12 (IL-12 stimulates the production of IL-10 in a negative feedback loop to regulate its own expression) and so the increased levels of IL-12 observed in Δ*YpTdp* infection may have contributed to higher levels of IL-10. Marginally lower levels of IFNγ were observed in the blood at 96 h during Δ*YpTdp* infection compared with wild-type infection (Fig. 6c). The appearance of IFNγ in blood samples corresponds to the appearance of both strains in the blood but the slightly higher levels of IFNγ in the wild-type infection may reflect the one mouse that achieved high titres of bacteria within the blood (Fig. 5). Further work is needed to correlate IFNγ levels with systemic infection and to confirm this difference between wild-type and mutant infection.

These findings may indicate that the immunomodulatory ability of *Y. pestis* Δ*YpTdp* may be somewhat altered compared with the wild-type *Y. pestis* GB but further investigations are required to confirm this. Nevertheless, any differences observed in the immunomodulation afforded by the strains do not significantly affect bacterial colonization in the infection models used in this study.

Because an obvious role in virulence could not be demonstrated for YpTdp using the infection models employed in this study, the *Y. pestis* Δ*YpTdp* deletion mutant was assessed for other phenotypes in a number of *in vitro* assays. Wild-type *Y. pestis* demonstrates an auto-aggregation phenotype

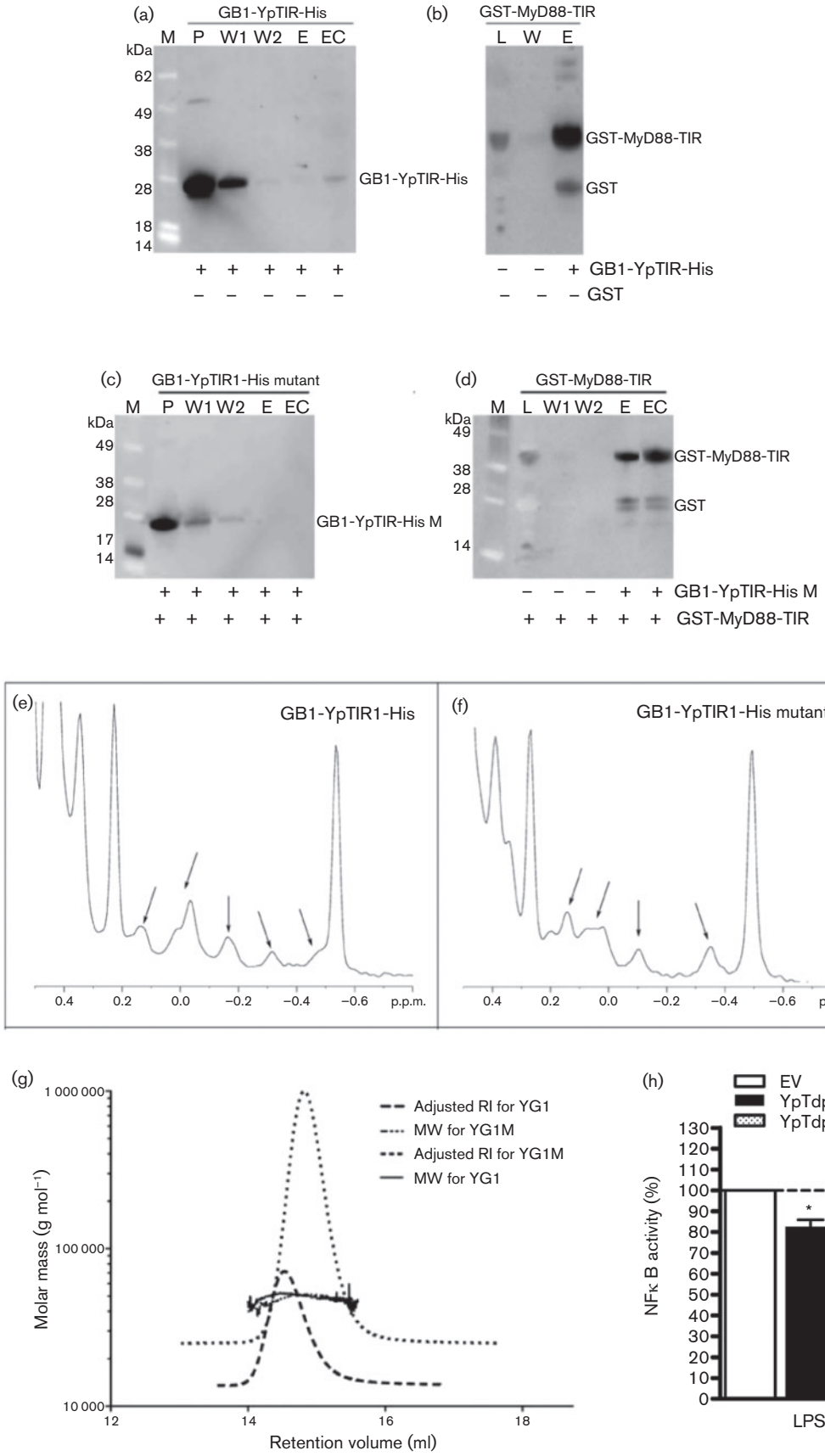
(a)
GB1-YpTIR-His
M P W1 W2 E EC
kDa
62
49
38
28
18
14
GB1-YpTIR-His
+ + + + +
– – – – –
(b)
GST-MyD88-TIR
L W E
GST-MyD88-TIR
GST
– – + GB1-YpTIR-His
– – – GST
(c)
GB1-YpTIR1-His mutant
M P W1 W2 E EC
kDa
49
38
28
17
14
GB1-YpTIR-His M
+ + + + +
+ + + + +
(d)
GST-MyD88-TIR
M L W1 W2 E EC
kDa
49
38
28
14
GST-MyD88-TIR
GST
– – – + + GB1-YpTIR-His M
+ + + + + GST-MyD88-TIR
(e)
GB1-YpTIR1-His
0.4 0.2 0.0 −0.2 −0.4 −0.6 p.p.m.
(f)
GB1-YpTIR1-His mutant
0.4 0.2 0.0 −0.2 −0.4 −0.6 p.p.m.
(g)
1 000 000
100 000
10 000
Molar mass (g mol⁻¹)
Adjusted RI for YG1
MW for YG1M
Adjusted RI for YG1M
MW for YG1
12 14 16 18
Retention volume (ml)
(h)
EV
YpTdp
YpTdp-P173H
130
120
110
100
90
80
70
60
50
40
30
20
10
0
NFκ B activity (%)
*
LPS

Fig. 4. Interaction between YpTIR and MyD88 is dependent on Pro173. Western blot analysis of samples obtained from GST pull-down experiments revealed a positive interaction between GB1-YpTIR-His and GST-MyD88-TIR (a, b) and a lack of interaction between the Pro173His mutant and GST-MyD88-TIR (c, d). Samples were probed with (a, c) anti-His antibody to detect the wild-type and mutant forms of GB1-YpTIR-His and (b, d) anti-GST antibody to detect GST-MyD88-TIR. M, molecular mass marker; P, protein; L, lysate; W, wash; E, eluate; EC, concentrated eluate. One-dimensional NMR analysis of the (e) wild-type and (f) Pro173His mutant forms of GB1-YpTIR1-His indicated that both forms of the YpTIR protein were folded. The peaks indicative of the folded state of the proteins are indicated by arrows. (g) Static light scattering measurements of the wild-type and Pro173His forms of GB1-YpTIR-His revealed that both proteins form dimers in solution. Measurements from the refractive index (RI) detector for the wild-type and Pro173His mutant forms of GB1-YpTIR1-His are shown as dotted and dashed lines, respectively. Data for the measured weight-average molecular masses for the wild-type and Pro173His mutant forms of GB1-YpTIR-His are shown as solid and broken lines, respectively. The measured molecular masses for the wild-type and Pro173His mutant forms of GB1-YpTIR-His are 50.7 and 49.9 kDa, respectively, while the predicted molecular mass of the monomeric form of GB1-YpTIR-His is 25.3 kDa. (h) A Pro173His mutant of YpTdp was constructed in the mammalian expression vector and used in LPS-induced TLR4 signalling experiments. HEK-Blue hTLR4 cells containing an alkaline phosphatase NFκB reporter were transfected with either empty vector or vector expressing YpTdp-P173H and stimulated with *E. coli* LPS (1 μg ml^{-1}) for 24 h. All results are expressed as percentage NFκB activity relative to stimulated cells transfected with empty vector (100 %). Results from previous YpTdp experiments (Fig. 2) are included for comparison. *$P<0.05$, column *t*-test.

when grown in broth at 28 °C, which has recently been attributed to the addition of complex sugars to surface proteins, and linked to the ability of *Y. pestis* to cause blockage of the flea stomach (Felek *et al.*, 2010). During growth of *Y. pestis* Δ*YpTdp* at 28 °C in BAB broth with orbital shaking, an increased auto-aggregation phenotype of *Y. pestis* Δ*YpTdp* was observed when compared with wild-type bacteria. This increased aggregation was quantified using a sedimentation assay in which the optical density of the culture was monitored over time with minimal disturbance (Fig. 7a). However, the increased auto-aggregation phenotype was not associated with a change in the hydrophobicity of the *Y. pestis* Δ*YpTdp* membrane, as reflected by its ability to bind to hydrocarbon (Fig. 7b), or with any change in its susceptibility to polymixin B (Fig. 7c), unlike the aggregation-deficient *pgmA* mutant (Felek *et al.*, 2010).

The *YpTdp* gene has been demonstrated to be upregulated in response to high salinity in two microarray studies (Han *et al.*, 2005, 2007). Therefore, *Y. pestis* Δ*YpTdp* was also tested for its ability to survive high NaCl concentrations (Fig. 7d). When incubated in 0.5 M NaCl for 3 h at 28 °C, survival of *Y. pestis* Δ*YpTdp* was reduced compared with the wild-type (2.5 % compared with 7.0 % for wild-type *Y. pestis*, $P=0.0238$ unpaired *t*-test), whereas there was no difference at 0.05 M NaCl, the approximate concentration of NaCl present in BAB broth. Taken together, these *in vitro* assessments of *Y. pestis* Δ*YpTdp* suggest that the YpTdp protein not only causes the bacteria to aggregate in larger clumps but also affects the ability of *Y. pestis* GB to regulate its osmolarity.

DISCUSSION

We have identified a TIR domain-containing protein, YpTdp, in the highly virulent bacterium *Y. pestis*. The protein is encoded by a gene in a region of recently acquired DNA, potentially via phage integration, adjacent to the *Y. pestis* HPI, in a region of low GC content. These regions of DNA are thought to be involved in adaptation from *Y. pseudotuberculosis* and encode proteins involved in *Y. pestis* survival within a host (Parkhill *et al.*, 2001).

Bacterial Tdps have been postulated to be involved in immune system evasion, disrupting TIR domain-dependent

Table 1. Virulence of *Y. pestis* Δ*YpTdp* via the subcutaneous route

Shown are the number of survivors and median time to death following different doses of *Y. pestis* GB and *Y. pestis* Δ*YpTdp* to calculate median lethal dose. Groups of six BALB/c mice were given a range of doses of *Y. pestis* GB or Δ*YpTdp* via the subcutaneous route. The mice were then monitored twice daily for 14 days and deaths recorded.

Dose*	*Y. pestis GB*			*Y. pestis ΔYpTdp*				
	10^{-7}	10^{-6}	10^{-5}	10^{-8}	10^{-7}	10^{-6}	10^{-5}	10^{-4}
No. of survivors (out of six)	1	0	0	5	2	0	1	0
Median time to death (days)	7	7	5.5	⩾14	9	7	6	5

*Dilution factor of 2×10^8 c.f.u. (ml culture)$^{-1}$.

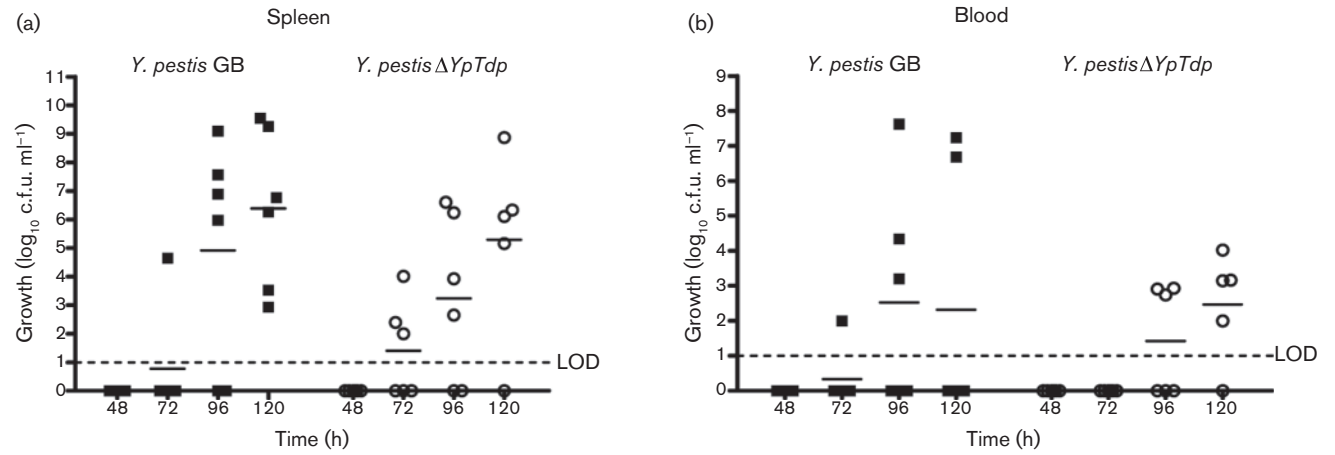

Fig. 5. Colonization of the spleen (a) and blood (b) by *Y. pestis* GB and *Y. pestis* Δ*YpTdp* in a murine model of infection. Eight groups of six BALB/c mice were inoculated with either 167 c.f.u. of *Y. pestis* GB or 125 c.f.u. of *Y. pestis* Δ*YpTdp* via the subcutaneous route. At 48, 72, 96 and 120 h post-challenge, two groups of mice were killed and bacterial load in the spleen and blood was enumerated by organ homogenization and serial dilution. Each point in the graphs represents a different mouse; the bar shows the mean of that group of six mice. LOD, limit of detection.

signalling pathways in order to dampen host immune responses long enough to reach a niche environment and establish infection. We have cloned the gene for expression of the *Y. pestis* TIR domain protein and assessed its ability to interfere with mammalian IL-1/TLR signalling. When overexpressed in HEK293 cells, YpTdp is able to disrupt IL-1β signalling through the IL-1R and to disrupt LPS signalling through TLR4. In contrast, YpTdp had no effect on the TIR-independent pathway from TNFα. When expressed alone, the TIR domain from YpTdp had no effect on any of these signalling pathways. There are a number of possible explanations for the lack of effect observed with YpTIR. For example, the disruption of signalling observed in the presence of YpTdp could be mediated by regions of YpTdp outside the TIR domain. However, the GST pull-down results reveal that there is an interaction between the GB1-YpTIR-His and GST-MyD88. Another possibility is that YpTIR expressed in mammalian cells is not folded or that it does not adopt precisely the same fold as in the full-length YpTdp. One-dimensional NMR analysis confirms that the YpTIR with a GB1 tag expressed in *E. coli* is folded. However, expression of YpTIR as a C-terminal His-tagged fusion in *E. coli* results only in very low amounts of folded protein. The presence of the GB1 tag was absolutely essential to the expression and isolation of soluble, stable protein in *E. coli*. This suggests that YpTIR-V5 expressed in mammalian cells is not correctly folded. A further possible explanation for the lack of effect of YpTIR on IL-1β signalling could be that YpTdp disrupts signalling by binding to human TIR domain proteins of the pathway, but that it is steric hindrance caused by the presence of the N- and C-terminal portions of the protein that blocks other TIR domain proteins from binding and thus prevents the formation of a signalling platform. The observed ability of YpTIR to bind a mammalian TIR domain (MyD88) coupled with the finding that this is not sufficient to inhibit the formation of a signalling platform in the cell-based assay correlates well with this suggestion. Attempts to investigate the direct interaction of YpTdp with MyD88 have been so far hampered by an inability to express high levels of YpTdp in either *E. coli* or HEK293 cells. Although YpTIR is able to interact with MyD88 it seems that full-length YpTdp is required for the disruption of signalling. YpTIR exists as a dimer in solution and, although its interaction with MyD88 is dependent on a single proline residue, its dimer formation is not. These data are consistent with the PdTIR structure. Knowledge of the structures of both the YpTIR and YpTdp alone and in complex with a human adaptor protein would provide greater insight into the function of the protein. The importance of Pro173 in YpTIR/YpTdp binding to MyD88 is further confirmed by the observation that a Pro173His mutation in YpTdp ameliorates its ability to downregulate LPS-induced signalling.

Following defined genetic deletion of YpTdp from *Y. pestis* GB, we observed no measurable effect on the virulence of this organism in its ability to colonize the spleen in competition with wild-type bacteria, based on its MLD in an injected BALB/c mouse model or its colonization of the spleen and blood over time in the same model. Levels of IL-12p70 and IL-10 in the spleen and of IFNγ in the blood during the colonization studies did show some differences between wild-type and mutant bacterial infection and may provide a starting point for the investigation into more subtle and co-operative effects that YpTdp may have on the innate immune response during *Y. pestis* infection. In addition, further *in vivo* studies using alternative models

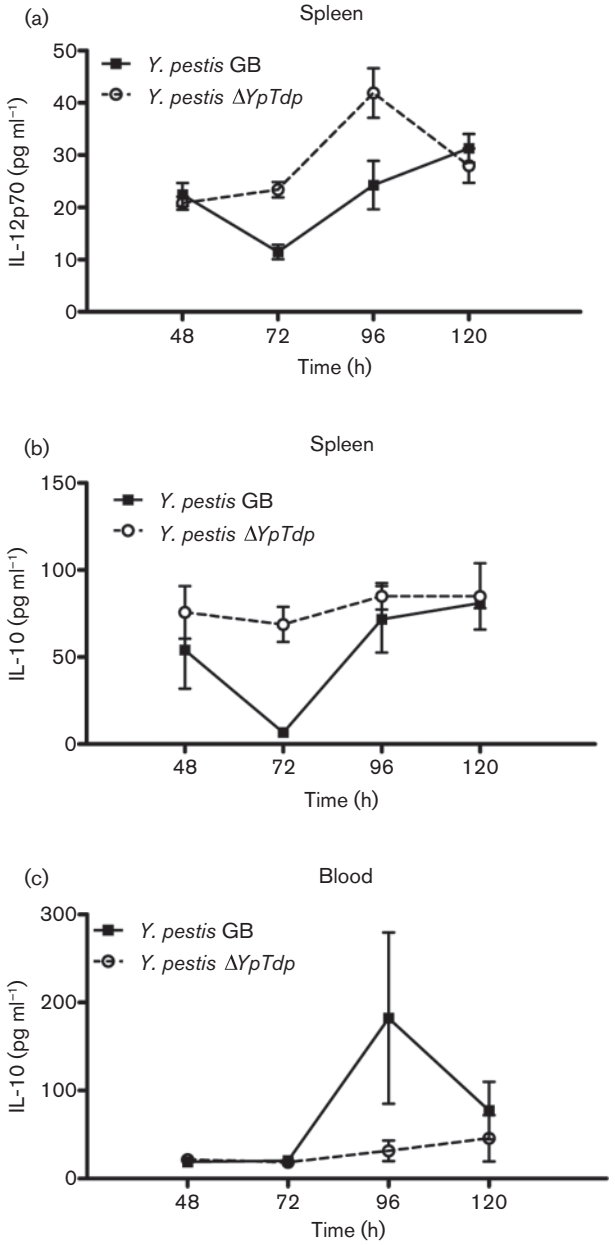

Fig. 6. Cytokine analysis from *Y. pestis* GB and *Y. pestis* Δ*YpTdp*-infected mouse spleens and blood. Eight groups of six BALB/c mice were subcutaneously administered with either 167 c.f.u. of *Y. pestis* GB or 125 c.f.u. of *Y. pestis* Δ*YpTdp*. At 48, 72, 96 and 120 h post-challenge two groups of mice were killed and their spleens were removed and homogenized. After centrifugation, the supernatants from these homogenates, or blood samples, were assessed for cytokine [IL-12p70 (a), IL-10 (b) and IFN-γ (c)] content.

and outputs of virulence may shed light on subtle *in vivo* effects produced by the removal of *YpTdp*. For example, the virulence of *Y. pestis* Δ*YpTdp* via the inhalational route, another natural route of infection for *Y. pestis*, has not been assessed in this study nor has the effect of *YpTdp* removal on colonization of the flea. The archetypal *Y. pestis* immunomodulatory protein YopJ also has limited effects on virulence when removed in isolation (Lemaître *et al.*, 2006).

Two phenotypes for the *Y. pestis* Δ*YpTdp* have been established *in vitro*. The *Y. pestis* Δ*YpTdp* mutant forms larger aggregates and sediments more rapidly than wild-type bacteria in broth culture. In addition, the *Y. pestis* Δ*YpTdp* mutant is unable to survive as well as wild-type *Y. pestis* in conditions of high salinity. These two phenotypes clearly warrant further investigation. Interestingly, in one study where *YpTdp* was shown to be upregulated under conditions of high salinity, the effect was abrogated in an *OmpR*-deficient background (Han *et al.*, 2007). As OmpR is a transcriptional regulator that controls the levels of the porins OmpC and OmpF in response to changes in osmoregularity (Yoshida *et al.*, 2006), it is possible to speculate that *YpTdp* expression is also regulated by OmpR, or that the dysregulation of osmoregularity control after removal of OmpR means the trigger for *YpTdp* to be upregulated at high salinity is lost.

It is clear that the *Y. pestis* Tdp can disrupt TIR-dependent mammalian immune signalling and is able to interact with MyD88 *in vitro*. The precise mechanism of action of YpTdp, and the range of pathways targeted, has yet to be fully characterized. It will be interesting to explore whether the YpTdp is able to inhibit MyD88-mediated upregulation by TLRs other than TLR4. This study shows that YpTdp can disrupt IL-1β and LPS signalling, but preliminary data suggest it does not affect zymogen-stimulated TLR2 signalling (data not shown). The majority of the data we have presented here indicate that YpTdp mediates its negative effects via competitive binding to MyD88, as suggested for the TIR domain from the uropathogenic *E. coli* strain CFT073, TcpC (Cirl *et al.*, 2008); however, the TIR domain from *Brucella melitensis*, TcpB, is thought to cause breakdown of the bridging adaptor MAL by an as yet uncharacterized mechanism (Sengupta *et al.*, 2010). These findings together with those presented here show that there is no one defined mechanism of action for negative regulation of TLR signalling of bacterial TIR proteins.

The assessment of the role of YpTdp in *Y. pestis* virulence in this study suggests that any effect on virulence is likely to be subtle or specific to a particular infection route or model. The *Y. pestis* Tdp-knockout mutant was not attenuated in its ability to colonize the spleen in competition with the wild-type when administered through the intravenous route, or attenuated in its lethality when given via the subcutaneous route. It was also not attenuated in its colonization of the spleen and blood when given via the subcutaneous route. This suggests that YpTdp is not a central virulence factor. Data on immunomodulatory proteins such as YopJ and the cytokine data from this study may suggest that the investigation of YpTdp as part of a co-ordinated immunomodulation strategy by *Y. pestis* is warranted.

Both our bioinformatic studies (Spear *et al.*, 2009) and the research presented here suggest that bacterial TIR domain

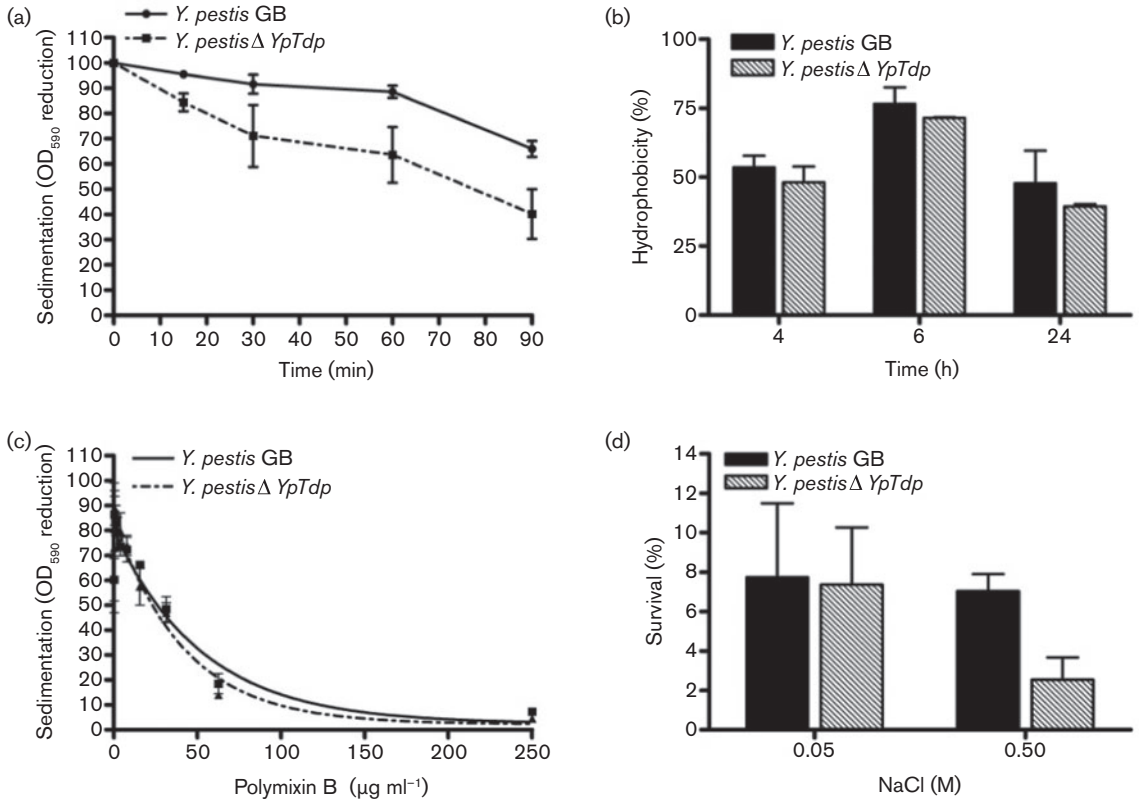

Fig. 7. Phenotypic evaluation of *Y. pestis* Δ*YpTdp.* (a) Increased auto-aggregation phenotype of *Y. pestis* Δ*YpTdp* as demonstrated by monitoring the sedimentation of the culture over time (associated with a reduction in optical density). Exponential phase cultures were analysed for sedimentation kinetics by repeated optical density reading at 590 nm. (b) Hydrophobic nature of *Y. pestis* GB and *Y. pestis* Δ*YpTdp* as investigated by the ability of each strain to bind n-hexadecane. Percentage hydrophobicity was assessed by the percentage change in OD_{590} of the aqueous phase before and after exposure to hydrocarbon. (c) Susceptibility of *Y. pestis* Δ*YpTdp* to polymixin B as measured by the percentage growth of cultures (OD_{590}) compared with the control. (d) Ability of *Y. pestis* Δ*YpTdp* to survive high-salinity shock. Exponential phase cultures were incubated with different NaCl concentrations for 3 h.

proteins may have other roles in addition to immune system evasion. Here, we demonstrate that the removal of YpTdp from *Y. pestis* causes an increase in auto-aggregation of the bacteria in broth culture, and an inability of the bacteria to survive in conditions of high salinity, which is also supported by other published studies. These phenotypes should now be more fully evaluated and the mechanism of action of YpTdp with respect to these phenotypes investigated. The data presented here provide some intriguing insights into the role of YpTdp. These findings have laid the foundations for further detailed analysis of the function and mechanism of action of this interesting protein.

It is still somewhat unclear whether the natural, or only, physiological role of bacterial TIR domain proteins is one of immune system evasion. It is clear from this study that the *Y. pestis* Tdp has the ability to disrupt TIR-dependent signalling, at least *in vitro*, but also possesses other functions. Our recent survey of bacterial Tdps found them to be promiscuous in their association with other domains and suggested a varied evolutionary history for these domains. Nature continually reuses established domains, with new functions emerging alongside suboptimal functions, and this may be the case for this *Y. pestis* TIR domain protein.

ACKNOWLEDGEMENTS

This work was funded by the UK Ministry of Defence. We gratefully acknowledge the provision of the NFκB and control luciferase reporter vectors by Professor Andrew Bowie, Trinity College, Dublin, Ireland. We also acknowledge the animal services staff at the Defence, Science and Technology Laboratory (Dstl), Salisbury, UK, for their assistance with the *in vivo* studies, and Dr Gregory Bancroft at the London School of Hygiene and Tropical Medicine and Dr Di Williamson at Dstl for their technical input.

REFERENCES

Airhart, C. L., Rohde, H. N., Bohach, G. A., Hovde, C. J., Deobald, C. F., Lee, S. S. & Minnich, S. A. (2008). Induction of innate immunity

by lipid A mimetics increases survival from pneumonic plague. *Microbiology* **154**, 2131–2138.

Balada-Llasat, J. M. & Mecsas, J. (2006). *Yersinia* has a tropism for B and T cell zones of lymph nodes that is independent of the type III secretion system. *PLoS Pathog* **2**, e86.

Beck, G., Puchelle, E., Plotkowski, C. & Peslin, R. (1988). Effect of growth on surface charge and hydrophobicity of *Staphylococcus aureus*. *Ann Inst Pasteur Microbiol* **139**, 655–664.

Buchrieser, C., Prentice, M. & Carniel, E. (1998). The 102-kilobase unstable region of *Yersinia pestis* comprises a high-pathogenicity island linked to a pigmentation segment which undergoes internal rearrangement. *J Bacteriol* **180**, 2321–2329.

Cirl, C., Wieser, A., Yadav, M., Duerr, S., Schubert, S., Fischer, H., Stappert, D., Wantia, N., Rodriguez, N. & other authors (2008). Subversion of Toll-like receptor signaling by a unique family of bacterial Toll/interleukin-1 receptor domain-containing proteins. *Nat Med* **14**, 399–406.

Datsenko, K. A. & Wanner, B. L. (2000). One-step inactivation of chromosomal genes in *Escherichia coli* K-12 using PCR products. *Proc Natl Acad Sci U S A* **97**, 6640–6645.

Deng, W., Burland, V., Plunkett, G., III, Boutin, A., Mayhew, G. F., Liss, P., Perna, N. T., Rose, D. J., Mau, B. & other authors (2002). Genome sequence of *Yersinia pestis* KIM. *J Bacteriol* **184**, 4601–4611.

Felek, S., Muszyński, A., Carlson, R. W., Tsang, T. M., Hinnebusch, B. J. & Krukonis, E. S. (2010). Phosphoglucomutase of *Yersinia pestis* is required for autoaggregation and polymyxin B resistance. *Infect Immun* **78**, 1163–1175.

Gay, N. J. & Keith, F. J. (1991). *Drosophila* Toll and IL-1 receptor. *Nature* **351**, 355–356.

Han, Y., Zhou, D., Pang, X., Zhang, L., Song, Y., Tong, Z., Bao, J., Dai, E., Wang, J. & other authors (2005). Comparative transcriptome analysis of *Yersinia pestis* in response to hyperosmotic and high-salinity stress. *Res Microbiol* **156**, 403–415.

Han, Y., Qiu, J., Guo, Z., Gao, H., Song, Y., Zhou, D. & Yang, R. (2007). Comparative transcriptomics in *Yersinia pestis*: a global view of environmental modulation of gene expression. *BMC Microbiol* **7**, 96.

Hinnebusch, B. J. (2005). The evolution of flea-borne transmission in *Yersinia pestis*. *Curr Issues Mol Biol* **7**, 197–212.

Huth, J. R., Bewley, C. A., Clore, G. M., Gronenborn, A. M., Jackson, B. M. & Hinnebusch, A. G. (1997). Design of an expression system for detecting folded protein domains and mapping macromolecular interactions by NMR. *Protein Sci* **6**, 2359–2364.

Latz, E., Verma, A., Visintin, A., Gong, M., Sirois, C. M., Klein, D. C., Monks, B. G., McKnight, C. J., Lamphier, M. S. & other authors (2007). Ligand-induced conformational changes allosterically activate Toll-like receptor 9. *Nat Immunol* **8**, 772–779.

Lemaître, N., Sebbane, F., Long, D. & Hinnebusch, B. J. (2006). *Yersinia pestis* YopJ suppresses tumor necrosis factor alpha induction and contributes to apoptosis of immune cells in the lymph node but is not required for virulence in a rat model of bubonic plague. *Infect Immun* **74**, 5126–5131.

Lukaszewski, R. A., Kenny, D. J., Taylor, R., Rees, D. G. C., Hartley, M. G. & Oyston, P. C. F. (2005). Pathogenesis of *Yersinia pestis* infection in BALB/c mice: effects on host macrophages and neutrophils. *Infect Immun* **73**, 7142–7150.

Maxson, M. E. & Darwin, A. J. (2004). Identification of inducers of the *Yersinia enterocolitica* phage shock protein system and comparison to the regulation of the RpoE and Cpx extracytoplasmic stress responses. *J Bacteriol* **186**, 4199–4208.

Medzhitov, R., Preston-Hurlburt, P. & Janeway, C. A., Jr (1997). A human homologue of the *Drosophila* Toll protein signals activation of adaptive immunity. *Nature* **388**, 394–397.

Monie, T. P., Moncrieffe, M. C. & Gay, N. J. (2009). Structure and regulation of cytoplasmic adapter proteins involved in innate immune signaling. *Immunol Rev* **227**, 161–175.

Newman, R. M., Salunkhe, P., Godzik, A. & Reed, J. C. (2006). Identification and characterization of a novel bacterial virulence factor that shares homology with mammalian Toll/interleukin-1 receptor family proteins. *Infect Immun* **74**, 594–601.

Nyman, T., Stenmark, P., Flodin, S., Johansson, I., Hammarström, M. & Nordlund, P. (2008). The crystal structure of the human toll-like receptor 10 cytoplasmic domain reveals a putative signaling dimer. *J Biol Chem* **283**, 11861–11865.

O'Neill, L. A. J. & Bowie, A. G. (2007). The family of five: TIR-domain-containing adaptors in Toll-like receptor signalling. *Nat Rev Immunol* **7**, 353–364.

Parkhill, J., Wren, B. W., Thomson, N. R., Titball, R. W., Holden, M. T. G., Prentice, M. B., Sebaihia, M., James, K. D., Churcher, C. & other authors (2001). Genome sequence of *Yersinia pestis*, the causative agent of plague. *Nature* **413**, 523–527.

Perry, R. D. & Fetherston, J. D. (1997). *Yersinia pestis*–etiologic agent of plague. *Clin Microbiol Rev* **10**, 35–66.

Poltorak, A., He, X., Smirnova, I., Liu, M. Y., Van Huffel, C., Du, X., Birdwell, D., Alejos, E., Silva, M. & other authors (1998). Defective LPS signaling in C3H/HeJ and C57BL/10ScCr mice: mutations in *Tlr4* gene. *Science* **282**, 2085–2088.

Radhakrishnan, G. K., Yu, Q., Harms, J. S. & Splitter, G. A. (2009). *Brucella* TIR domain-containing protein mimics properties of the Toll-like receptor adaptor protein TIRAP. *J Biol Chem* **284**, 9892–9898.

Rana, R. R., Simpson, P., Zhang, M., Jennions, M., Ukegbu, C., Spear, A. M., Alguel, Y., Matthews, S. J., Atkins, H. S. & Byrne, B. (2011). *Yersinia pestis* TIR-domain protein forms dimers that interact with the human adaptor protein MyD88. *Microb Pathog* **51**, 89–95.

Reed, L. J. & Muench, H. (1938). A simple method of estimating fifty per cent endpoints. *Am J Hyg* **27**, 493–497.

Robinson, V. L., Oyston, P. C. & Titball, R. W. (2005). A dam mutant of *Yersinia pestis* is attenuated and induces protection against plague. *FEMS Microbiol Lett* **252**, 251–256.

Rosenberg, M. (1984). Isolation of pigmented and nonpigmented mutants of *Serratia marcescens* with reduced cell surface hydrophobicity. *J Bacteriol* **160**, 480–482.

Salcedo, S. P., Marchesini, M. I., Lelouard, H., Fugier, E., Jolly, G., Balor, S., Muller, A., Lapaque, N., Demaria, O. & other authors (2008). *Brucella* control of dendritic cell maturation is dependent on the TIR-containing protein Btp1. *PLoS Pathog* **4**, e21.

Schubert, S. R., Rakin, A. & Heesemann, J. (2004). The *Yersinia* high-pathogenicity island (HPI): evolutionary and functional aspects. *Int J Med Microbiol* **294**, 83–94.

Sengupta, D., Koblansky, A., Gaines, J., Brown, T., West, A. P., Zhang, D., Nishikawa, T., Park, S.-G., Roop, R. M., II & Ghosh, S. (2010). Subversion of innate immune responses by *Brucella* through the targeted degradation of the TLR signaling adapter, MAL. *J Immunol* **184**, 956–964.

Sims, J. E., March, C. J., Cosman, D., Widmer, M. B., MacDonald, H. R., McMahan, C. J., Grubin, C. E., Wignall, J. M., Jackson, J. L. & other authors (1988). cDNA expression cloning of the IL-1 receptor, a member of the immunoglobulin superfamily. *Science* **241**, 585–589.

Spear, A. M., Loman, N. J., Atkins, H. S. & Pallen, M. J. (2009). Microbial TIR domains: not necessarily agents of subversion? *Trends Microbiol* **17**, 393–398.

Stubben, C. J., Duffield, M. L., Cooper, I. A., Ford, D. C., Gans, J. D., Karlyshev, A. V., Lingard, B., Oyston, P. C., de Rochefort, A. & other authors (2009). Steps toward broad-spectrum therapeutics: discovering virulence-associated genes present in diverse human pathogens. *BMC Genomics* **10**, 501.

Taylor, V. L., Titball, R. W. & Oyston, P. C. (2005). Oral immunization with a dam mutant of *Yersinia pseudotuberculosis* protects against plague. *Microbiology* **151**, 1919–1926.

Triantafilou, M., Gamper, F. G., Haston, R. M., Mouratis, M. A., Morath, S., Hartung, T. & Triantafilou, K. (2006). Membrane sorting of toll-like receptor (TLR)-2/6 and TLR2/1 heterodimers at the cell surface determines heterotypic associations with CD36 and intracellular targeting. *J Biol Chem* **281**, 31002–31011.

Xu, Y. W., Tao, X., Shen, B. H., Horng, T., Medzhitov, R., Manley, J. L. & Tong, L. (2000). Structural basis for signal transduction by the Toll/interleukin-1 receptor domains. *Nature* **408**, 111–115.

Yadav, M., Zhang, J., Fischer, H., Huang, W., Lutay, N., Cirl, C., Lum, J., Miethke, T. & Svanborg, C. (2010). Inhibition of TIR domain signaling by TcpC: MyD88-dependent and independent effects on *Escherichia coli* virulence. *PLoS Pathog* **6**, e1001120.

Yoshida, T., Qin, L., Egger, L. A. & Inouye, M. (2006). Transcription regulation of ompF and ompC by a single transcription factor, OmpR. *J Biol Chem* **281**, 17114–17123.

Zhou, D. S. & Yang, R. F. (2009). Molecular Darwinian evolution of virulence in *Yersinia pestis*. *Infect Immun* **77**, 2242–2250.

Edited by: P. H. Everest